Northumbria Research Link

Radio-based Device-free Activity Recognition with Radio Frequency Interference

Bo Wei[†‡], Wen Hu[†‡] ,Mingrui Yang[‡], Chun Tung Chou[†]
[†] School of Computer Science and Engineering,
University of New South Wales, Sydney, NSW, Australia
[‡] CSIRO, Brisbane, Queensland, Australia
{bwei,ctchou, wenh}@cse.unsw.edu.au[†]
{mingrui.yang}@csiro.au[‡]

ABSTRACT

Activity recognition is an important component of many pervasive computing applications. Device-free activity recognition has the advantage that it does not have the privacy concern of using cameras and the subjects do not have to carry a device on them. Recently, it has been shown that channel state information (CSI) can be used for activity recognition in a device-free setting. With the proliferation of wireless devices, it is important to understand how radio frequency interference (RFI) can impact on pervasive computing applications. In this paper, we investigate the impact of RFI on device-free CSI-based location-oriented activity recognition. We conduct experiments in environments without and with RFI. We present data to show that RFI can have a significant impact on the CSI vectors. In the absence of RFI, different activities give rise to different CSI vectors that can be differentiated visually. However, in the presence of RFI, the CSI vectors become much noisier and activity recognition also becomes harder. Our extensive experiments shows that the performance of state-of-the-art classification methods may degrade significantly with RFI. We then propose a number of counter measures to mitigate the impact of RFI and improve the location-oriented activity recognition performance. Our evaluation shows the proposed method can improve up to 10% true detection rate in the presence of RFI. We also study the impact of bandwidth on activity recognition performance. We show that with a channel bandwidth of 20 MHz (which is used by WiFi), it is possible to achieve a good activity recognition accuracy when RFI is present.

1. INTRODUCTION

Activity recognition aims to identify what a subject is doing. It is an important component of many pervasive computing applications. For example, the increasing greying population in many countries puts a rising pressure on the health care system. Activity recognition can be used to improve home care for the elderlies. This paper considers the activity recognition problem using radio signals, in the device-free setting, with an emphasis on making activity recognitions robust to radio frequency interference (*RFI*).

Activity recognition is a well researched topic. In terms of system components, there are three broad approaches to the activity recognition problem: camera-based [19, 7, 42, 4, 16], sensor-based [12, 3, 21, 8, 35, 6, 40] and device-free [29, 27]. Cameras are able to provide high resolution data for activity recognition but privacy is a serious concern. Although there is no privacy concern with the sensor-based approach, it imposes the requirement that a subject has to carry sensors on his body. This is inconvenient and activity recognition fails if the subject forgets to carry the device. We have therefore chosen the device-free approach in this paper.

In the device-free approach to activity recognition, radio devices are placed in the periphery of a monitored area, called the area of interest (AoI). These radio devices send packets to each other regularly and use the received radio signal to obtain information on the radio environment. The key idea is that the radio environment is influenced by the activity taking place in the AoI. The activity recognition problem is to infer the activity from the received radio signal. In general, there are *three requirements* for device-free activity recognition: *informative measurements*, *capability to deal with environment changes*, and *robustness to RFI*.

Using informative measurements is a pre-requisite for any successful classification problem. Although coarse-grained radio channel measurements, such as radio signal-strength indicators (RSSI), have been successfully used for device-free indoor localisation [41, 32, 30], they are no longer informative for activity recognition. Recent work on device-free activity recognition [29, 27] has therefore used Channel Frequency Response (CFR) or Channel State Information (CSI) for activity recognition. This is also our observation and our proposed solution therefore uses CSI.

A challenge for CSI-based device-free activity recognition is that the CSI of the radio channel is sensitive to changes in the environment due to for example new or moved furniture. This is because the CSI-fingerprint of an activity is affected by multi-path effects of the environment. A recent work in CSI-based activity recognition called E-eyes [29] proposed a semi-supervised approach to address the issue of environmental changes. When the system detects that the CSI-fingerprint for an activity has changed, E-eyes requires the users to label the new CSI-instances manually. A similar approach was used in [24] to deal with the impact of

environmental changes on CSI-based localisation.

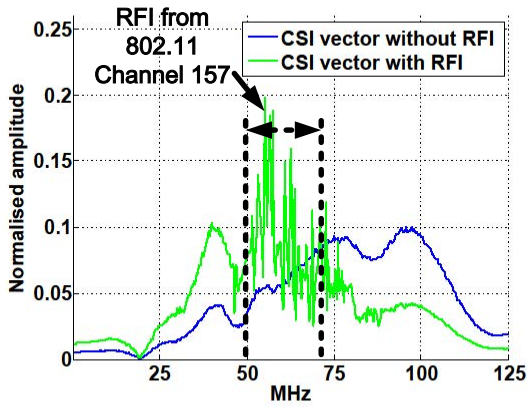

Figure 1: CSI without and with RFI.

Another challenge for CSI-based activity recognition is that the CSI is highly influenced by RFI. The number and types of radio devices have proliferated in the last decade. It is hardly possible to find a frequency band that is clean or without RFI. Our observation, which is depicted in Fig. 1, shows that CSI is **highly impacted** by RFI. The figure shows a CSI without RFI as well as a CSI with RFI in a particular radio channel. The impact of RFI on CSI is conspicuous. This implies that CSI-based activity recognition must be robust to RFI. This is the key topic of this paper, and it does not appear to have been addressed before.

As a summary of the above discussion, we have drawn a Venn diagram with the three requirements of informative measurements, robustness to environmental changes, and robustness to RFI in Fig. 2. This diagram is used to differentiate our work (indicated by a star) from two other recent CSI-base activity recognition solutions: E-eyes [29] and Sigg et al. [27]. It shows which solution is able to deal with which requirements. Two important remarks are appropriate here. First, neither of [29, 27] addresses the impact of RFI on CSI. Second, our proposed solution can use the semi-supervised approach of [29] to deal with the impact of environmental changes. This means our proposed solution can deal with all the three requirements.

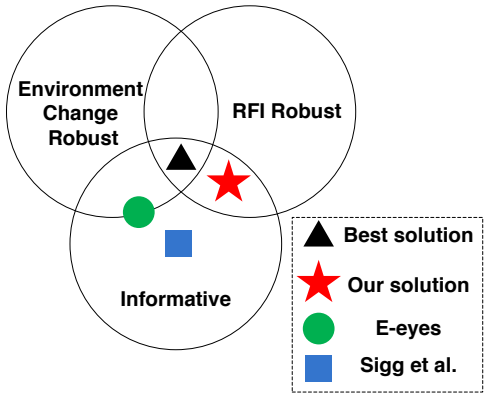

Figure 2: Differentiating our work from other recent work on CSI-based activity recognition.

In order to improve the robustness of CSI-based activity classification, we exploit the state-of-the-art Sparse Representation Classification (SRC) approach based on ℓ_1-optimisation. SRC has been shown to be robust to noise. It has also been shown to significantly improve the classification performance in face recognition [33, 26] and acoustic classification [31], outperforming other classification approaches such as support vector machine (SVM) and k-nearest neighbours (kNN). In this paper, we propose a new SRC-based classification method to improve the robustness of CSI-based location-oriented activity recognition. Location-oriented activity recognition is able to indicate the location information as well as types of activities.

To summarise, the contributions and novelties of this paper are:

- We demonstrate by using real measurements that CSI is highly impacted by RFI. We show that, while the CSI vectors for different activities in a RFI-free environment are clearly distinguishable even by naked eyes, this is no longer the case for an environment with RFI.
- To address the above challenge, we propose a novel SRC-based classification algorithm for CSI-based location-oriented activity recognition. The algorithm fuses the results from a number of ℓ_1-optimisation according to their signal-to-noise ratios (SNRs). We show that this method can boost recognition accuracy and outperforms kNN and other SRC-based methods by up to 10%.
- We study the impact of channel bandwidth on the accuracy of activity recognition. We use 4 different bandwidths: 5, 10, 15 and 20 MHz, which cover low bandwidth devices (e.g. ZigBee) and high bandwidth devices (e.g. WiFi). We show that our proposed classification algorithm produces good classification accuracy for activities with 20 MHz of bandwidth.

The rest of this paper is organised as follows. Section 2 presents background materials on CSI and SRC. We then study the impact of RFI on CSI and propose our CSI-based activity recognition method in Section 3. Next, we present evaluation results in Section 4 using experimental data collected from an apartment. Section 5 presents related work. Finally, Section 6 concludes the paper.

2. BACKGROUND

2.1 Wireless Platform and Channel State Information

We use a platform called Wireless Ad hoc System for Positioning (WASP) [22] for our experiments. The WASP nodes are originally designed for high resolution localisation and use a much wider bandwidth than many off-the-shelf wireless devices. WASP can operate in both 2.4 GHz and 5.8 GHz industrial, scientific and medical (ISM) bands, using a bandwidth of, respectively, 83 MHz and 125 MHz. WASP uses Orthogonal Frequency-Division Multiplexing (OFDM) at the physical layer and time division multiple access (TDMA) at the media access control (MAC) layer. In fact, the physical layer of WASP is realised by using commercial off-the-shelf IEEE 802.11 radio chips.

OFDM is a multi-carrier modulation technique. At the 5.8 GHz band, the WASP nodes use 320 sub-carriers. Each

of these sub-carriers has a different centre frequency. This means the received sub-carriers at two frequencies can experience different amount of phase shifts, giving different frequency response. For a sub-carrier with centre frequency f_i, the complex channel response $C(f_i)$ is related to the transmitted symbol $T(f_i)$ and received symbol $R(f_i)$ by $R(f_i) = C(f_i)T(f_i)$. The complex number $C(f_i)$ captures both relative change in signal amplitude and phase shift. Let $f_1, f_2, ..., f_{320}$ denote the centre frequencies of the 320 sub-carriers that WASP nodes use. Then the CSI is a complex vector $[C(f_1), C(f_2), ..., C(f_{320})]$. Since we will only be using the *amplitude* of CSI for classification and in order to keep the language simple, we assume that CSI is the real vector $[|C(f_1)|, |C(f_2)|, ..., |C(f_{320})|]$. More details about CSI can be found in [39].

2.2 Sparse Representation Classification

Sparse Representation Classification (SRC) is first proposed in [33] for face recognition. It has subsequently been applied to other areas, such as acoustic classification [31] and visual tracking [14]. A key feature of SRC is its use of ℓ_1 minimisation to make the classification robust to noise.

We give a brief description of SRC here, the details can be found in [33]. We assume that the classification problem has s classes. Class i is characterised by the sub-dictionary $D_i = [d_{i1}, ..., d_{in_i}]$ where d_{ij} $(j = 1, ..., n_i)$ are the n_i feature vectors derived from training data. For classification, the s sub-dictionaries are concatenated to form a dictionary $D = [D_1, D_2, ..., D_s]$. Ideally, a test sample y should sit in a subspace spanned by the dictionary, i.e. there exists a *coefficient vector* x such that $y = Dx$. However, due to noise, such an x cannot be found or is perturbed. Instead, the SRC method solves for the coefficient vector x using the following ℓ_1 optimisation problem:

$$\hat{x} = \arg\min_x \|x\|_1 \quad \text{subject to } \|y - Dx\|_2 < \epsilon, \qquad (1)$$

where ϵ is the noise level. Note that instead of requiring that $y = Dx$, the constraint requires only that the vectors y and Dx are sufficiently close to each other. The estimated coefficient vector $\hat{x}$ is used for the classification algorithm. Note that the length of $\hat{x}$ is $\sum_{i=1}^{s} n_i$. Let $\hat{x}_i$ denote the n_i-dimension sub-vector in $\hat{x}$ that corresponds to the sub-dictionary D_i. We calculate the residual $r_i = \| y - D\hat{x}_i \|_2$ for Class i. The class that gives the minimum residual is returned as the classification result.

SRC has a main superiority: featureless. This provides us an opportunity to build a training set from the CSI measurements rather than extracting feature from them. Moreover, SRC is known to be robust to noise. As our work is to study the performance of activity recognition when RFI is present, we investigate how to explore SRC to boost SNR for improving recognition performance.

3. ACTIVITY RECOGNITION USING CSI

This section presents our method to recognise a set of location-oriented activities using CSI in the device-free setting. We first demonstrate that CSI is influenced by activities taking place in a room and can be used to identify the location-oriented activity. We demonstrate the challenge of CSI based activity recognition when RFI is present. Finally, we present our SRC based classification method which takes RFI into consideration.

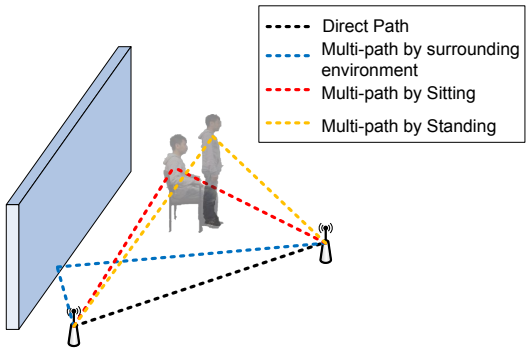

(a) Examples of multiple paths caused by different activities

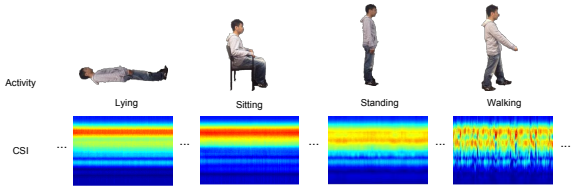

(b) Examples of CSI vectors cause by different activities

Figure 3: Examples of multiple paths and CSI vectors (Best view in colour)

3.1 CSI contains location-oriented activity information

We first present some intuition on why device-free CSI-based location-oriented activity recognition is possible. Fig. 3(a) depicts an indoor environment with two wireless nodes and the multi-paths that the radio propagation may take. It shows that different multi-path effects can be obtained if a person is sitting or standing. Its results in different CSI vectors at the receiver and can be used to identify the activity (shown in Fig. 3(b)). Furthermore, different locations of a monitored person also differentiate multi-paths, *which makes location-oriented activity recognition feasible.*

In order to demonstrate the feasibility of CSI-based activity recognition, we set up two WASP nodes in an apartment with one living room and one bedroom. The nodes are 5 metres apart with 3 walls in the line-of-sight path between the nodes. The subject is positioned in an AoI between the two nodes but is not in the direct path between the 2 nodes. The subject carry out 4 different activities: sitting, lying, standing, and walking. A WASP node is used as the transmitter and the other as a receiver. The transmitter sends to the receiver at 10 packets per seconds, and it needs a 2.5 milliseconds slot to send a packet. This means only *2.5% of running time* is occupied for sending data for activity recognition, which does not occupy bands too much to affect the radio communication of other wireless devices. For each packet received, the receiver uses the WASP interface to obtain the CSI vector and SNR for that packet. It is also important to point out that the data in this experiment is collected in a *clean* environment without any RFI.

Fig. 5(a) shows the normalised CSI vectors under the four different activities. The horizontal axis shows the sample number where a sample corresponds to a packet. There are 320 values in the vertical axis which corresponds to the 320

sub-carriers. The magnitude of the CSI is shown as a heat plot. We have put four blocks of data side-by-side in the figure, which corresponds to the four activities of lying, sitting, standing and walking. It can readily be seen that the four activities have highly distinguishable CSI. This confirms that CSI contains information on activity. Another observation is that the CSI fluctuates a lot when the subject is walking. This is due to different multi-path effects created by the person walking. Fig. 5(a) shows the CSI when a 125 MHz bandwidth is used. We now show that the same observations also apply when we use a 20 MHz channel. The box in Fig. 5(a) is Channel 157 in the 802.11 standards with 20 MHz bandwidth. We have enlarged the CSI in the box and plotted it in Fig. 5(b). It can be seen that the CSI for the four activities are very distinguishable and walking creates more fluctuations in CSI.

Fig. 5(c) shows the SNR of the corresponding samples (packets). It shows that the SNR has a slightly larger fluctuation when the subject is walking. However, there does not appear to be any noticeable differences in the SNR data series among lying, sitting, and walking. These observations suggest that it may be possible to use SNR to distinguish between walking from the other three activities where the subject is stationary. However, it does not seem to be possible to use SNR to distinguish between the three stationary activities.

Since CSI is sensitive to the multi-path effect, same activity in different locaitons can have different CSI. Training in each interesting location must be performed for location-orientated activity recognition, and this is a limitation of CSI-based finger-printing activity recognition. Fig. 4 demonstrates the different CSI as a result of the same activity "standing" in two locations. This fact requires additional training for same activity in different locations, but it helps location-orientated activity recognition systems locate activities. [37, 36, 29, 27, 15] also apply a similar strategy, i.e. conducting training in various locations, for improving the performance of radio-based pattern recognition.

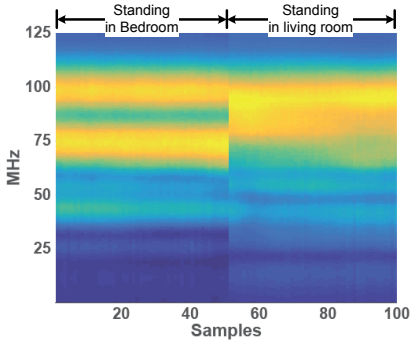

Figure 4: CSI of standing in different locations.

3.2 Challenges of CSI-based activity recognition

The above results are obtained when the two WASP nodes are in a clean environment without RFI. We conduct another experiment using the same set up but we add a pair of IEEE 802.11a devices that communicates in Channel 157 (a 20 MHz band). Our goal is to understand the impact of RFI on CSI and SNR.

Fig. 5(d) shows the CSI for the four activities when RFI is present in Channel 157. It shows that the CSI in Channel 157 (enclosed by the white rectangle) is fairly noisy but the four activities still have distinguishable CSI outside of Channel 157. This suggests that if wide-band devices are used to obtain the CSI for activity recognition, then we can use the part of CSI with little RFI to identify the activity. *However, with ubiquitous use of wireless technologies such as WiFi, Bluetooth, IEEE 802.15.4, etc., it becomes more and more difficult or even impossible to find RFI-free bandwidth, particularly in ISM bands, for radio-based activity recognition systems. We therefore consider the possibility of using CSI in an interfered channel to perform activity recognition.*

In order to examine the effect of RFI, we plot the CSI of Channel 157 in Fig. 5(e). It shows that the CSI vectors of different activities are no longer highly distinguishable. However, if we look closer at the CSI vectors of each activity, we can see that a number of CSI vectors among one activity are almost the same. This recurrence of CSI vectors suggests that we may use a block of CSI vectors for classification instead of individual CSI vectors. However, this classification is going to be challenging because the CSI vectors appear to be fairly noisy. We will propose a few different classification methods in Section 3.3 to address this challenge.

We now examine the impact of RFI on SNR. Fig. 5 shows the SNR of the four activities when RFI is present in Channel 157. We see that the SNR of all four activities are highly fluctuating. We suggested earlier that it would be possible to tell walking from the static activities using SNR when RFI is absent, however, this does not appear to be feasible once RFI is present.

To sum up, it is a challenge to use CSI to perform activity recognition when RFI is present.

3.3 Location-oriented Activity Recognition with RFI

We now describe our proposed CSI-based activity recognition in the presence of RFI. The goal of activity recognition is to identify four daily activities: sitting, standing, lying and walking in different rooms, as well as whether the AoI is empty.

3.3.1 Data collection and pre-processing

Our method fingerprints the activities using CSI vectors. The first procedure is to record the CSI measurements for building a training set, and use the training set to fingerprint the test data by using our proposed machine learning algorithm.

For each CSI vector in a training set or a test set, we first apply exponential smoother to remove the high frequency noise and decrease the noise level. However, exponential smoother cannot take effect for all CSI vectors when experiencing high SNR. Therefore, we still need further mechanism to improve the recognition performance.

Besides, RFI causes the unexpected change to CSI vectors. There is no existing model for the performance of CSI vector under RFI. Therefore, we need to consider the RFI environment when training the dictionary. In other words, the CSI vectors of one specific activity under different physical or radio environments vary significantly. We have to update training set for a new RFI environment. The method in [29] can be applied for updating the dictionary when RFI

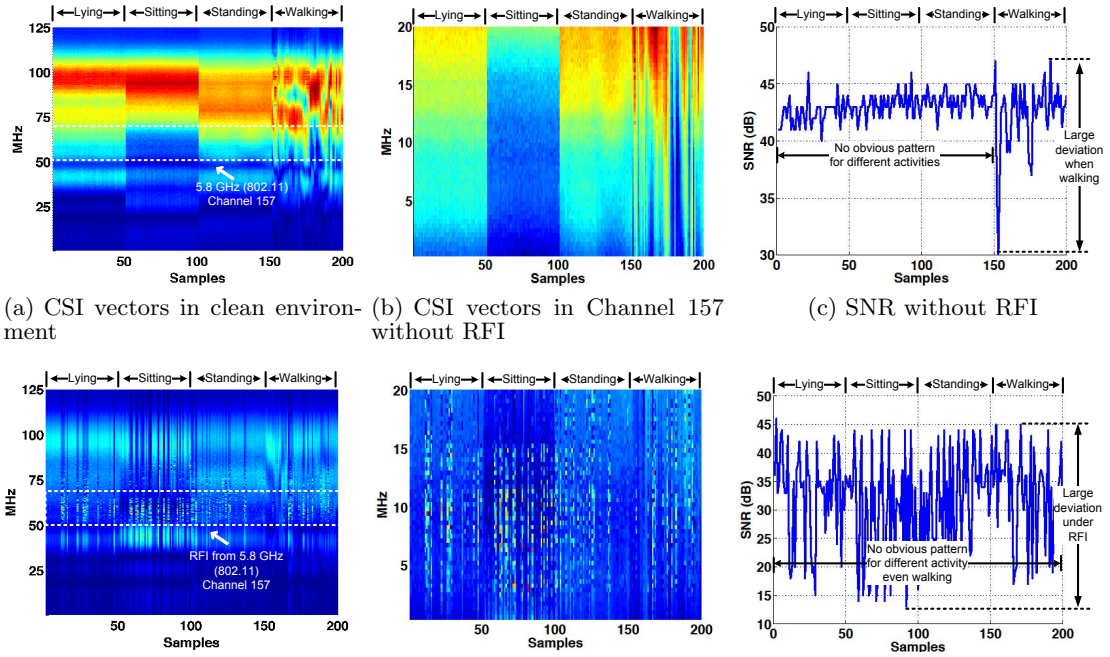

(a) CSI vectors in clean environment (b) CSI vectors in Channel 157 without RFI (c) SNR without RFI

(d) CSI vectors in RFI environment (e) CSI vectors in Channel 157 with RFI (f) SNR with RFI

Figure 5: CSI and SNR performance in different activities (Best view in colour)

is present.

3.3.2 *Classification algorithms*

We have seen that RFI causes the CSI vector to be very noisy. In order to deal with RFI, we introduce a window size ws where ws consecutive CSI vectors are used for classification. One possible method is to stack ws CSI vectors into a long feature vector and use it for classification. However, this will be computationally intensive because the feature vector has a very high dimension. Instead, we will use the one CSI vector at a time and investigate different fusion methods.

Let $y_1, y_2, ..., y_{ws}$ denote the CSI vectors in the time window, and D be the dictionary. We first solve the following ℓ_1-optimisation problem for $i = 1, .., ws$:

$$\hat{x}_i = \arg\min_x \|x\|_1 \quad \text{subject to } \|y_i - Dx\|_2 < \epsilon, \qquad (2)$$

We now present three different fusion methods which use $\hat{x}_i$ $(i = 1, .., ws)$ in different ways.

The first method is to use decision fusion and will be referred to as $\ell_1 - voting$. For this method, the algorithm uses each $\hat{x}_i$ to arrive at a decision class using the standard SRC algorithm described in Section 2.2. This method then uses majority voting to arrive at a decision.

The second method is to fuse the $\hat{x}_i$ vectors by computing their mean: $\hat{x}_{\text{sumup}} = \frac{1}{ws}\sum_{i=1}^{ws} \hat{x}_i$. The mean vector $\hat{x}_{\text{sumup}}$ is then use to compute the residuals for each class as in the standard SRC algorithm described in Section 2.2. This method returns the class that minimises the residual. Note that this fusion method was proposed by Misra et al. in [18] where they shown that such method could improve the GPS recovery accuracy. We will call this method ℓ_1-*sumup*.

The method ℓ_1-*sumup* applies equal weights to all $\hat{x}_i$ by computing a simple average of them. However, it is possible that some CSI vectors in the window are less affected by noise. This can also be seen from Fig. 5 where the SNR fluctuates. We therefore propose to use SNR of a sample to derive a weighting for that sample. Let S_i denote the SNR of the i-th sample in the window. We compute the weighted mean of $\hat{x}_i$ using:

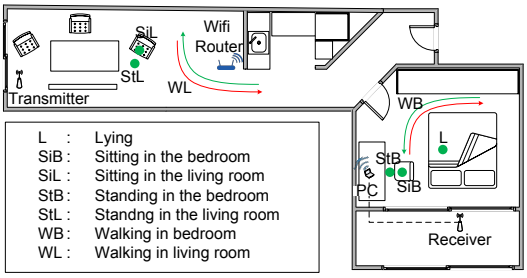

Figure 6: Floor plan of the experiment environment

$$\hat{x}_{\text{weighting}} = \sum w_i \hat{x}_i, \qquad (3)$$

$$w_i = \frac{A_i}{\sum_{j=1}^{ws} A_j}, \quad A_i = 10^{(\frac{S_i}{20})}, \qquad (4)$$

The mean vector $\hat{x}_{\text{weighting}}$ is then use to compute the residuals for each class as in the standard SRC algorithm described in Section 2.2. This method returns the class that minimises the residual. We call this method as ℓ_1-*weighting*.

4. EVALUATION

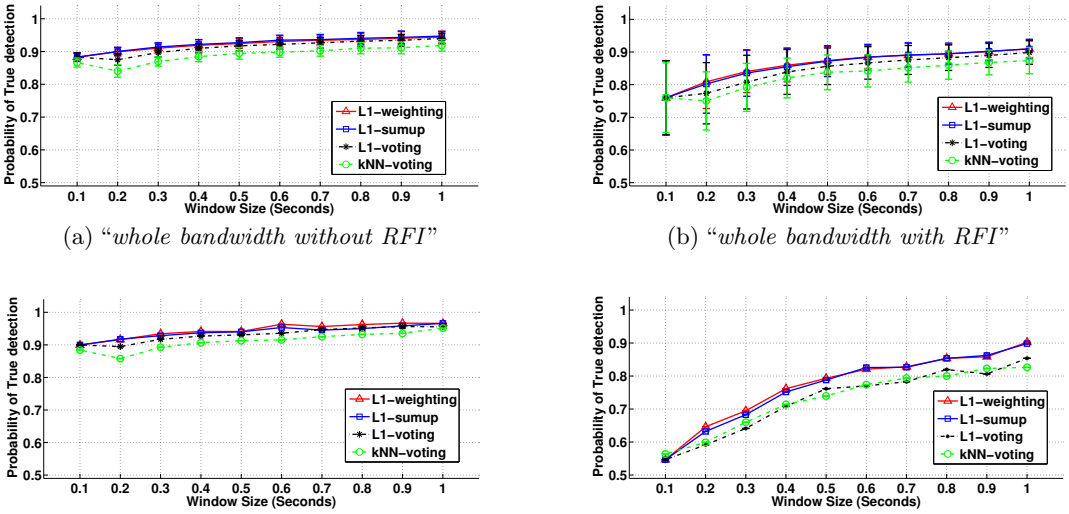

(a) "*whole bandwidth without RFI*" (b) "*whole bandwidth with RFI*"

(c) "*Channel 157 without RFI*" (d) "*Channel 157 with RFI*"

Figure 7: The Performance vs Window Size

4.1 WASP nodes

We use a pair of WASP nodes in our experimental evaluation. We provided some basic information on WASP nodes in Section 2.1. We provide further background information and explain some design choices here.

We choose WASP because it is a software-defined radio and there is an API to obtain CSI. WASP can operate in both 2.4 GHz and 5.8 GHz. We choose to perform our evaluation in 5.8 GHz because this band is less used compared to the 2.4 GHz band. It is therefore easier to find places where RFI is absent across the entire 125 MHz bandwidth that WASP operates in. This allows us to do two things. First, we can experiment in a clean radio frequency (RF) environment and use CSI from the clean environment to establish benchmark for the classification algorithm. Second, this allows us to control the amount of RFI present in our experiments and we can be sure that any RFI present in the environment is added by us. We can therefore study the impact of RFI on activity recognition. Another reason for choosing the 5.8 GHz band is that WASP nodes have a bandwidth of 125 MHz in this band. This allows us to emulate protocols with wider bandwidth, e.g. 80 MHz bandwidth for 802.11ac.

WASP is a low-power wireless platform. The energy cost is 2 W when WASP is receiving beacons, and 2.5 W when transmitting. A pair of WASP nodes only consumes 4.5 W [22]. WASP nodes can be powered by cable, which means the deployment of a pair of WASP nodes for activity recognition only cost no more than 4 kWh per month.

4.2 Experiment Setup

The experiment is conducted in an apartment whose floor plan is shown in Fig. 6. The AoI includes one living room (top half of the floor plan) and one bedroom (the room on the right). Two WASP nodes are deployed at the edge of the AoI. One node works as the transmitter and sends a beacons once every 0.1 second. This node is near the left-hand end of the apartment and is marked as transmitter in the floor plan. The other WASP node acts as a receiver and this is where the CSI data is collected. This node is located in the balcony just outside the bedroom. This node is marked as the receiver in the floor plan. The receiver is connected to a computer (labelled as PC in the floor plan) in the bedroom and this computer is the sink for the CSI data. The distance between the transmitter and receiver is about 5 metres.

We consider 8 different location-oriented activity classes: (1) E: empty environment (2) L: lying on the bed in the bedroom (3) SiB: sitting in the bedroom (4) SiL: sitting in the living room (5) StB: standing in the bedroom (6) StL: standing in the living room (7) WB: walking in the bedroom (8) WL: walking in the living room. The location of the activities are marked in the floor plan in Fig. 6. We perform standing and sitting in the same location, because we want to also focus on activity classification without considering different locations to evaluate the efficiency of our method. We also differentiate sitting and standing in different locations for evaluating the location-oriented activity recognition. We believe the proposed recognition method can also be applied to other activities by training. In this section, we only evaluate the most common activities in the daily life. For each activity class, CSI data is collected for 1 minute, so that no physical environmental changes take place during this time. For a given data set, we have 600 CSI samples for each location-oriented activity, resulting in $600 \times 8 = 4,800$ CSI samples in total.

We use a computer (PC) and a WiFi router to create RFI in the environment. Their locations are marked in the floor plan in Fig. 6. They use 802.11a protocol, which operates in 5.8 GHz, to communicate in Channel 157 (a 20 MHz channel). The computer communicates with the router using the echo request `ping` command as fast as possible with the default packet size 7 kilobytes; the router responses the request with echo reply packet containing the exact data of request packet. The average transmission rate will arrive at more than 30 Mbit/s. In order to simulate the RFI that the activity recognition system may actually experience, we place the WiFi router in the middle of the apartment, which is a natural location that people will use in order to provide

Table 1: Bandwidth for different wireless protocols

Wireless Protocol	Bandwidth per Channel	Number of Subcarrier in OFDM
2.4 GHz (ZigBee)	5 MHz	13
2.4 GHz (802.11b/g/n)	20 MHz	52
3.6 GHz (802.11y)	5/ 10/ 20 MHz	13/ 26/ 52
4.9 GHz (802.11y)	20 MHz	52
5 GHz (802.11a)	20 MHz	52
5 GHz (802.11n)	20/ 40 MHz	52/ 104
5 GHz (802.11ac)	20/ 40/ 80 MHz	52/ 104/ 208

WiFi coverage to their apartment. The distance between the WiFi router and the receiver is about 4 metres, but in one experiment, the router is moved to different locations to create different amount of RFI at the receiver. The distance between the PC and the receiver is about 1.5 metres.

4.3 Evaluation methodology and metrics

We apply 10-fold cross validation to each data set to evaluate our proposed method. The results from the 10 folds are averaged to obtain the final result. We use both the probability of true detection and confusion matrix to present our results.

We have two *primary* data sets. One data set is collected under clean environment while the other is collected when there is RFI in Channel 157. We use these data sets to investigate the effect of bandwidth on location-oriented activity recognition. In particular, we investigate what happens if we use a bandwidth of 5 MHz, 10 MHz, 15 MHz, 20 MHz, 40 MHz, 80 MHz and 125 MHz. Let us assume that we use a bandwidth window size B MHz where B is one of 5, 10, 15, 20, 40, 80 or 125. Recalling that WASP nodes have a bandwidth of 125 MHz. We first select the first B MHz of the 125 MHz-band and use the sub-carriers in the B MHz to perform classification. We then shift the bandwidth window by 5 MHz. If a *complete* B MHz can be found in the data, we perform another calculations. We iterate until the whole 125 MHz is covered. We will refer to the results obtained by sliding bandwidth window over the 125 MHz band as "*whole bandwidth without RFI*" and "*whole bandwidth with RFI*".

Instead of using the whole 125 MHz in the primary data sets. We also created two *secondary* data sets, from the with and without RFI cases, which include over those subcarriers in Channel 157. These secondary data sets span a bandwidth of 20 MHz. Note that, when interference sources exist, all sub-carriers in the secondary data sets are with RFI while only some of the sub-carriers in the primary data sets are with RFI. In other words, the secondary data sets are worst case scenario with RFI. By using the secondary data sets, we investigate what happens when we use a bandwidth window of 5 MHz, 10 MHz, 15 MHz, 20 MHz. The methodology of shifting the bandwidth window is the same as that for primary data sets. We will refer to the results obtained from the secondary data sets as "*Channel 157 without RFI*" and "*Channel 157 with RFI*".

Our classification algorithm uses a window size of ws consecutive CSI samples for classification, as discussed in Section 2.2. We will also vary this window size in our investigation.

We consider the following 4 classification algorithms: kNN with majority voting (kNN-*voting*), ℓ_1-*voting* , ℓ_1-*sumup* and ℓ_1-*weighting*. In order to demonstrate the improvement in using a window size ws, we sometimes also show the result of using one CSI sample or a window size of 1; we will use "kNN-*win*1" and "ℓ_1-*win*1" to denote the algorithms that use a $ws = 1$. Sigg et al. compared the performance of kNN and decision tree for radio-based device-free activity recognition and showed kNN had better behaviour [27]. Therefore, we compare our proposed method with kNN in this section.

4.4 Effect of Window Size

In this section, we study the impact of window size ws on location-oriented activity recognition performance. We use ws from 1 to 10, which correspond to a time of 0.1 s and 1 s, because the transmitter sends beacons at a frequency of 10 Hz. We will show that window size can improve accuracy but this is at the expense of decreasing the temporal resolution of activity recognition. We will use both primary data sets ("*whole bandwidth without RFI*" and "*whole bandwidth with RFI*") and both secondary data sets ("*Channel 157 without RFI*" and "*Channel 157 with RFI*") in this study. We assume a bandwidth window size $B = 20$, which is the bandwidth of one 5.8 GHz 802.11 channel.

First, we discuss the performance of using "*whole bandwidth without RFI*". Fig. 7(a) shows the probability of true detection of the 4 different algorithms. When there is no RFI and with a 20 MHz bandwidth window size, a window size ws of 1 can already achieve an accuracy of approximately 90% for all four classification algorithms. The accuracy gradually increases to 95% when the window size is increased to 10. The results are similar if we use "*Channel 157 without RFI*", as shown in Fig. 7(c). The algorithms ℓ_1-*weighting*, ℓ_1-*sumup* and ℓ_1-*voting* show similar performance but are slightly better than kNN$-$*voting*. This shows that, without RFI, very good classification accuracy can be obtained.

As we discussed earlier, the challenge is to perform classification when there is RFI. Fig. 7(b) shows the probability of true detection for the data set "*whole bandwidth with RFI*". It shows that the performance increases with larger window size. Among the four algorithms used, ℓ_1-based algorithms outperform kNN and the best performing algorithms are ℓ_1-*weighting* and ℓ_1-*sumup*. If we compare the classification accuracy between the without and with RFI in Fig. 7(a) and 7(b), we see a significant drop in accuracy when RFI is present especially when the window size is small. For example, for $ws = 1$, accuracy decreases from 90% to 76% because of RFI. We now turn to the data set "*Channel 157 with RFI*". Again, larger window size means better accuracy, and both ℓ_1-*weighting* and ℓ_1-*sumup* perform the best. The most telling observation is that, for $ws = 1$, the classification accuracy is merely 57% but if $ws = 10$ is used, an accuracy of almost 90% can be obtained. This shows that window size can have a significant effect on performance when RFI is present.

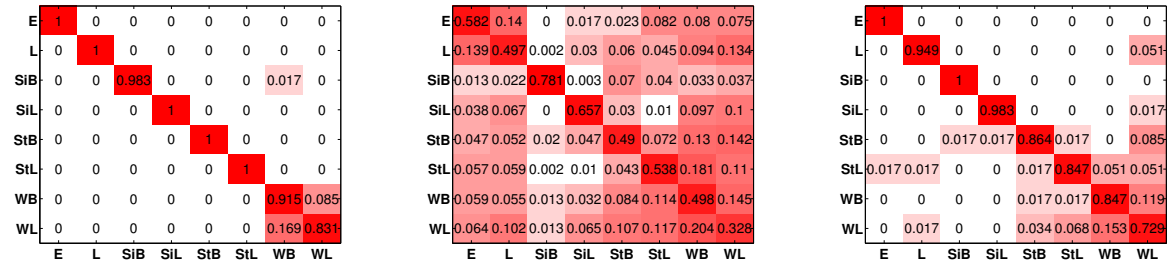

(a) $ws = 10$ and $B = 20$ MHz in "*Channel 157 without RFI*" (b) $ws = 1$ and $B = 20$ MHz in "*Channel 157 with RFI*" (c) $ws = 10$ and $B = 20$ MHz in "*Channel 157 with RFI*"

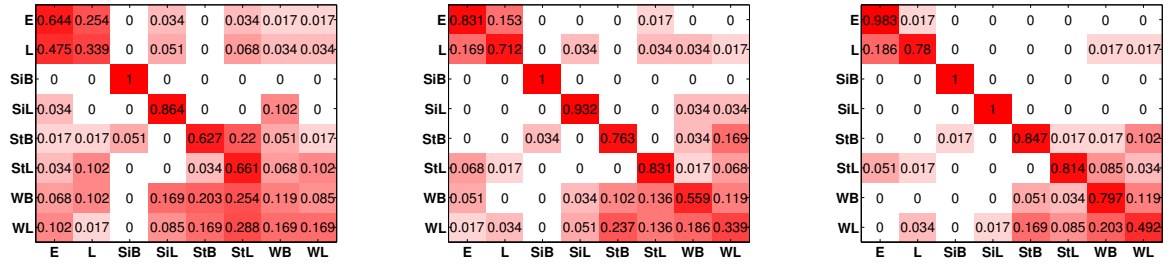

(d) $ws = 10$ and $B = 5$ MHz in "*Channel 157 with RFI*" (e) $ws = 10$ and $B = 10$ MHz in "*Channel 157 with RFI*" (f) $ws = 10$ and $B = 15$ MHz in "*Channel 157 with RFI*"

Figure 8: Confusion Matrix vs different settings

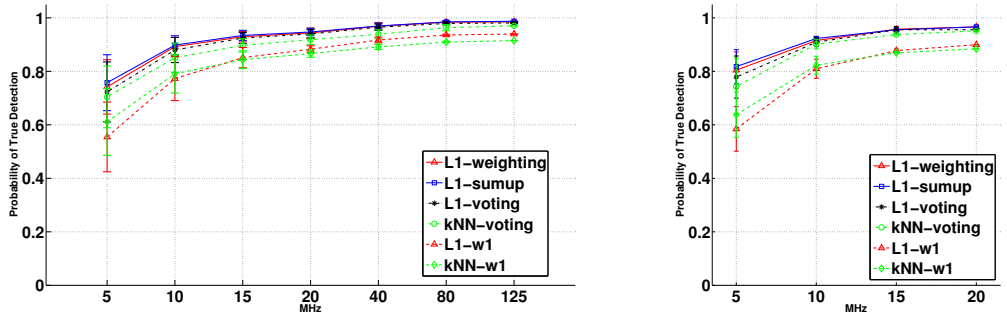

(a) "*whole bandwidth without RFI*" (b) "*Channel 157 without RFI*"

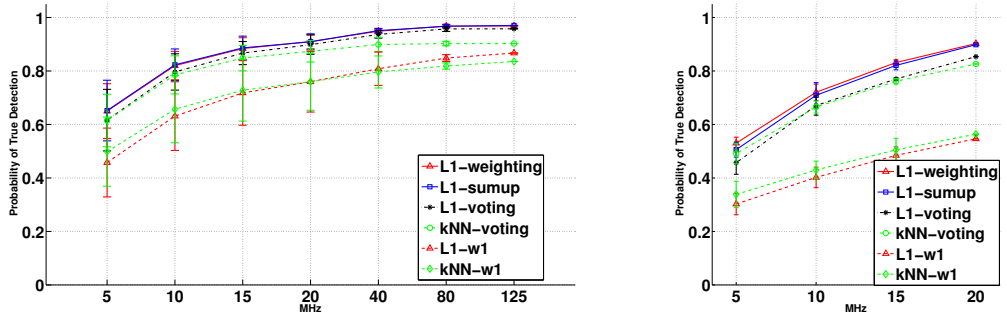

(c) "*whole bandwidth with RFI*" (d) "*Channel 157 with RFI*"

Figure 9: The performance vs bandwidth window size

We now present the confusion matrices for location-oriented activity recognition using our proposed ℓ_1-*weighting*. Fig. 8(a) shows the confusion matrix for "*Channel 157 without RFI* with a window size of 10 (1 second). It shows that perfect accuracy is achieved with 5 activities. The accuracy for static activities is extremely high. The accuracy for the two walking activities are also very good. We now present the confusion matrix for "*Channel 157 with RFI*" with a window size of 0.1 second and 1 second, in respectively, Fig. 8(b) and 8(c). It can be seen that a big window size has significantly improved classification accuracy of many activities. In the following sections, we will use a default window size $ws = 10$ (1 second).

4.5 Effect of the Bandwidth Window Size

In this section, we discuss the influence of the bandwidth window size on the location-oriented activity recognition performance. This study takes advantage of the available wide bandwidth from WASP nodes to simulate different kinds of protocols shown in Table 1.

The result of using different bandwidth window size B for data set "*whole bandwidth without RFI*" is shown in Fig. 9(a). As expected, increasing B gives a better classification accuracy. In particular, ℓ_1-*weighting* achieves an accuracy of 75%, 95% and 97% when using a bandwidth window B of 5 MHz, 20 MHz and 125 MHz respectively. Similar trend is also observed for the data set "*Channel 157 without RFI*" (shown in Fig. 9(b)). The algorithms ℓ_1-*weighting*, ℓ_1-*sumup* and ℓ_1-*voting* show similar performance, which are slightly better than kNN-*voting*.

Fig. 9(c) shows the probability of true detection for the data set "*whole bandwidth with RFI*". It shows the performance increases when the bigger bandwidth window size increases. Comparing four algorithms using window size ws 10, ℓ_1-*weighting* and ℓ_1-*sumup* perform the best. When using a bandwidth window B greater than or equal to 20 MHz, the performance of ℓ_1-*voting* is close to that of ℓ_1-*weighting* and ℓ_1-*sumup*, all outperform kNN-*voting*. When looking at the data set "*Channel 157 with RFI*" (shown in Fig. 9(d)), the accuracy decreases significantly, especially when the bandwidth window sizes B are 5 MHz and 10 MHz whose accuracy decreases from 82% and 90% to 55% and 70% using ℓ_1-*weighting* compared with the data set "*Channel 157 without RFI*". In the data set "*Channel 157 with RFI*", the performance of ℓ_1-*weighting* and ℓ_1-*sumup* is close, but they show their superiority over ℓ_1-*voting* and kNN-*voting*, for example, the accuracy of ℓ_1-*weighting* and ℓ_1-*sumup* is 5% better than ℓ_1-*voting* and kNN-*voting* when the bandwidth window size B is 20 MHz. This shows ℓ_1-*weighting* and ℓ_1-*sumup* algorithms increase the recognition performance when there is RFI.

Fig. 8(d), Fig. 8(e), Fig. 8(f) and Fig. 8(c) illustrate the confusion matrix using ℓ_1-*weighting* with the bandwidth window size B 5 MHz, 10 MHz, 15 MHz and 20 MHz respectively in the data set "*Channel 157 with RFI*". It shows that the using larger bandwidth window size B helps increase the accuracy and robustness to RFI. When the bandwidth window size B is 20 MHz, 2 static activities have perfect accuracy, 2 static activities have accuracy more than 90%, and 2 static activities along with "walking in the bedroom" have accuracy more than 80%.

4.6 Effect of Different Distances Between the Router and Receiver

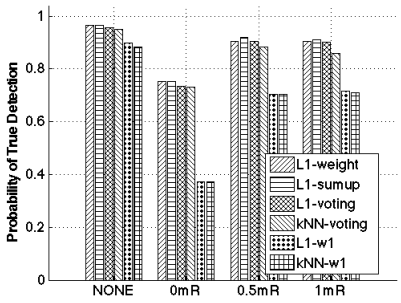

Figure 10: The performance influenced by the distances between the router and the receiver

In order to evaluate the impact of the amount of interference on classification. We vary the distance between one interferer (the WiFi router in the floor plan in Fig. 6) and the WASP receiver. We consider 4 cases: no interference (NONE), interferer just next to the the receiver (0mR), 0.5 metre away from the receiver (0.5mR), and 1 metre away form the receiver (1mR). The classification uses only Channel 157. The computer also communicates with the router using the echo request `ping` command as fast as possible.

Fig. 10 shows the influence of receiver-interferer distance on the probability of true detection. It shows that for 0mR, the accuracy can drop by more than 10%. However, by using a window size $ws = 10$, ℓ_1-*weighting* has an accuracy about 80%. Note that there is not much difference between the 0.5mR and 1mR cases. Also, there is only a slight drop in performance for the ℓ_1 algorithms between NONE and 0.5mR cases. This shows that if an interferer is not present within 0.5m of the receiver, then the activity recognition accuracy is still high.

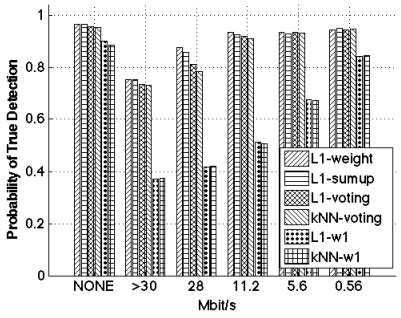

Figure 11: The performance under different transmission rates between the router and the receiver

4.7 Effect of Different traffic Between Interference Source and Receiver

In this section, we study the effect of traffic sending rates on the classification performance. We keep one interference source (the WiFi router in the floor plan in Fig. 6) next to the receiver and adjust the `ping` rates of the interferer. The `ping` rate is set to "as fast as possible" (average transmission rate more than 30 Mbit/s), 500 packets per second (transmission rate 28 Mbit/s), 200 packets per second(transmission rate 11.2 Mbit/s), 100 packets per second (transmission rate 5.6 Mbit/s) and 10 packets per second (transmission rate 0.56 Mbit/s). These settings roughly cor-

Table 2: Features for SNR based walking detection

Feature	Equation
Standard Deviation	$\sigma = \frac{1}{n-1}\sqrt{E[(S(k)-\mu)^2]}$
Peak	$\rho = max(S) - min(S)$
Head Size	$\eta = max(S) - median(S)$
3rd Order Central moment	$\gamma = E[(S(k)-\mu)^3]$

respond to the bit rates of watching online videos with frame rates 1080p, 480p and 360p, which give rise to bit rates of 8 Mbit/s, 5 Mbit/s and 1 Mbit/s respectively.

Fig. 11 shows the classification performance under different transmission rates. Our proposed ℓ_1-*weighting* method reaches 90% accuracy when transmission rate is 28 Mbit/s, which means it is robust to the transmission rate 28 Mbit/s. In contrast, the accuracy of both ℓ_1-*voting* and kNN-*voting* algorithm is no more than 90%. *This means our proposed ℓ_1-weighting is more robust to RFI than the other methods.* Moreover, ℓ_1-*weighting* achieves an accuracy of 97% when the transmission rate is 11.2 Mbit/s. The accuracy stays almost the same for lower transmission rates.

4.8 SNR based Walking Detection Discussion

In Section 3, we discuss the possibility of using SNR to differentiate walking from non-walking, i.e. a detection or binary classification problem. We see from Fig. 5(c) that, when RFI is absent, this is probably feasible because walking gives rise to highly fluctuating RSI while non-walking does not. However, in the presence of RFI, the distinction between walking and non-walking is not so conspicuous, as seen in Fig. 5(f). In this section, we want to investigate what classification performance we can get if we use SNR for walking detection. This study is also motivated by the fact that many device-free localisation methods [43, 9, 44] use SNR as a feature to find the location of the person in AoI.

The detection problem is to detect whether the person is walking. This covers the classes of WL and WB instead of walking detection with location information. A commonly used feature for device-free localisation is the variance of the SNR, which is used in for example [43]. However, in order to minimise the possibility that walking detection fails due to poor choice of features, we have chosen to use 4 different features listed in Table 2: Standard Deviation, Peak, Head Size, and 3rd Order Central moment where S is SNR vectors and μ is the mean of SNR values in a vector. For training, we use a logistic regression model.

The alternative to using SNR for walking detection is to use CSI with ℓ_1 classifier. We will compare these two methods. The comparison uses 10-fold cross validation and measurements from Channel 157. We consider two data sets, "*Channel 157 without RFI*" and "*Channel 157 with RFI*".. Also, for both data sets, we use bandwidth window sizes B of 5 MHz, 10 MHz and 20 MHz bands.

Since walking detection is binary classification, we use the following metrics:

True Positive Rate (TPR): $TPR = TP/(TP+FN)$
False Positive Rate (FPR): $FPR = FP/(FP+TN)$
F1 score: $F1\ score = 2TP/(2TP+FP+FN)$

where TP, TN, FP and FN are the number of true positives, true negatives, false positives, and false negatives respectively.

Table 3 shows the comparison between detection using SNR and using CSI. Each column illustrates one bandwidth window size B in each data set and we highlight the better statistics. A number of observations can be made: (1) In the absence of RFI, detection using SNR has a higher TPR compared to using CSI for a bandwidth window of 5 MHz; however, for a bandwidth window of 10 or 20 MHz, detection using CSI has a higher TPR. (2) In the absence of RFI, it is viable to use either SNR or CSI based detector for walking detection. (3) RFI causes the performance of both detectors to decrease. However, the SNR-based detector has a sharper drop in TPR. (4) Overall, the CSI-based detector is more robust in the presence of RFI.

5. RELATED WORK

We have already discussed the most related work, i.e. work on using CSI for activity classification, in Section 1. In this section, we discuss work in three areas: activity recognition, pattern recognition from radio data and the application of compressed sensing in wireless networks.

5.1 Activity recognition

Activity recognition forms the basis of many context aware pervasive computing applications. We can broadly classify activity recognition according to whether they are sensor-based or camera-based. Many sensor-based activity recognition systems have been proposed. Acceleration sensor is one of the most frequently used sensors [12, 3, 21]. This is because miniature acceleration sensors are cheap and readily available, and they can be found on all smartphones. For example, Keally et al. [10] used sensors smartphone as well as sensors wore on wrists, ankles and head to distinguish between walking, cycling, sitting and other activities. Recently, a number of wristbands, that are equipped with acceleration sensor, are available in the market. Products such as Jawbone Up [8] and Xiaomi Mi Band [35] can achieve good activity recognition accuracy but they require the users to wear the devices.

Microphone is another sensor that has been used in activity recognition. Hao et al. [6] present a method to monitor sleep quality using microphone; however, it is not sure whether the same method will function in daily activity recognition in a noisy environment. Yatani and Truong [40] designed a wearable acoustic sensor which can be used to record the sound near the throat of the user, and use the measurements for activity recognition. Again, the issue is that the subject has to wear a sensor.

Cameras are also widely used for activity recognition, localisation and tracking [19, 7, 42, 4, 16, 13, 25]. An advantage of camera sensors is that they free the subjects the need to wear or to remember to wear a device. Another advantage is that they provide very rich data which can be used to distinguish between many different activities. However, the Achilles' heel of using camera for activity recognition is privacy concern. Also, cameras can only cover a limited area. For monitoring in an apartment, a camera is needed in each room. On the contrary, activity recognition using radio signals can cover a much wider area and can "see" through walls, while cameras cannot. We have therefore chosen to use device-free radio-based activity recognition which does not need subjects to carry a device and has no privacy concerns.

5.2 Radio based pattern recognition

The propagation of radio waves in an environment is af-

Table 3: Performance of walking detection (Better statistics in each column is highlighted)

	Without RFI			With RFI		
Bandwidth	5 MHz	10 MHz	20 MHz	5 MHz	10 MHz	20 MHz
TPR (SNR)	**0.8496**	0.9463	0.9661	0.3305	0.4576	0.6356
FPR (SNR)	0.0254	**0.0151**	0.0085	**0.0501**	**0.0631**	0.0650
F1 score (SNR)	**0.8790**	0.9514	0.9708	0.3980	0.5427	0.6848
TPR (CSI)	0.7627	**0.9802**	**1**	**0.4237**	**0.6695**	**0.9237**
FPR (CSI)	**0.0148**	0.0160	**0.0028**	0.1165	0.0866	**0.0424**
F1 score (CSI)	0.8441	**0.9666**	**0.9958**	**0.4779**	**0.8225**	**0.9008**

fected by the objects and people in the environment, through reflection, diffraction, constructive and destructive interference and so on. There is much interest in using the received signal characteristics to infer about the attributes of people and objects in an environment. The received signal characteristics used can be coarse or fine grained.

An example of coarse grained radio signal feature is RSSI which measures the received signal power. RSSI has been successfully used in device-free localisation [32, 43, 9, 44, 30, 38]. This is because a person standing in an area between the transmitter and receiver can attenuate, reflect, scatter the radio waves. These effects create a characteristic pattern in RSSI which can be used to infer the location of people in the environment.

Unfortunately, only limited information on the environment can be inferred from RSSI. There is a growing interest to use fine grained features of radio signals for inference. This is also fuelled by the availability of API to query CSI from WiFi chipsets such as Intel 5300 [5] and Atheros 9390 [23]. CSI has been used for many pattern recognition problems, including localisation [24], human detection [45], activity recognition [29, 27], fine-grained gesture recognition [15] and to "lip-read" [28]. As mentioned in Section 1, our work differs from earlier work on using CSI for activity recognition in that we take RFI into consideration while earlier work did not.

Radio signals have also been used to perform gesture recognition. WiSee designed by Adib et al. [2] and WiVi designed by Pu et al. [20] used software-defined radio to extract the Doppler effect caused by the gesture. In order to reduce energy consumption, Kellogg et al. [11] built AllSee which uses RFID tags and power-harvesting sensors for gesture recognition. However, these work can only recognise dynamic gestures and are not able to detect static activities because they rely on Doppler effect. To further improve the resolution of the radio signal based localisation and gesture recognition, Adib et al. [1] designed WiTrack and obtain time-of-flight from the Frequency Modulated Carrier Wave (FMCW) technology for localisation in 3 dimensions. Witrack has high resolution for localisation (approximately 10 cm), but needs to use a bandwidth of 1.69 GHz. However, we show in this paper as few as 20 MHz of bandwidth can be used to distinguish static activities with good accuracy. Moveover, none of these works designed their systems with RFI, while our work takes RFI into consideration.

5.3 Application of Compressed Sensing on Wireless Sensor Networks

Recently, compressed sensing has been applied to wireless sensor networks. SRC proposed by Wright et al. [33] is one of the applications of compressed sensing which helps increase the recognition performance. Wei et al. [31] developed an acoustic classification method on wireless sensor networks by applying SRC to increase the recognition performance and decrease the computation time to meet the requirement of real-time classification. Shen et al. [26] optimised the random matrix used for SRC to boost the face recognition performance in smartphones.

Besides recognition, compressed sensing is also applied to background subtraction [25], data compression for in-situ soil moisture sensing [34], and cross-correlation for acoustic ranging [17] and GPS ranging [18].

Compared with these works, this paper is the first to investigate the feasibility of SRC for radio-based activity recognition. Furthermore, our work also takes advantage of SRC for activity recognition with RFI in present.

6. CONCLUSIONS

In this paper, we investigate the performance of radio based device-free location-oriented activity recognition systems under RFI, and propose a novel fusion algorithm based on SRC that can improve the recognition performance of the systems by up to 10% when RFI is present. Our prototype robust location-oriented activity recognition systems require only one pair of nodes for a one-bedroom apartment, which enables easy system set-up and maintenance. Finally, we use an embedded wide band radio device (WASP platform) to emulate and study the recognition performance of popular wireless communication protocols that have different bandwidths under RFI. For future work, we plan to investigate the performance of other radio-based pattern recognition applications, e.g. gesture recognition [2, 20, 11], 3D localisation [1], with RFI. We will also discuss more factors of RFI influence for activity recognition. kNN with weighting strategy is also an interesting topic for the future work. Radio-based activity recognition in any location without additional training is an open question as well.

Acknowledgements. We thank our shepherd, Dr. Mark Coates, and the anonymous reviewers for their helpful feedbacks on earlier versions of this paper. We also thank Phil Ho, Mark Hedley, Sandeep Goli, Adrian Bonchis and Weitao Xu for their help when we used WASP nodes at the early stage.

7. REFERENCES

[1] F. Adib, Z. Kabelac, D. Katabi, and R. C. Miller. 3D tracking via body radio reflections. In *NSDI '14*, Seattle, WA, 2014.

[2] F. Adib and D. Katabi. See through walls with WiFi! In *SIGCOMM '13*, pages 75–86, New York, NY, USA, 2013. ACM.

[3] L. Bao and S. S. Intille. Activity recognition from user-annotated acceleration data. In *Pervasive computing*, pages 1–17. Springer, 2004.

[4] I. Cohen and H. Li. Inference of human postures by classification of 3D human body shape. In *AMFG 2003.*, pages 74–81. IEEE, 2003.

[5] D. Halperin, W. Hu, A. Sheth, and D. Wetherall. Tool release: Gathering 802.11n traces with channel state information. *ACM SIGCOMM CCR*, 41(1):53, Jan. 2011.

[6] T. Hao, G. Xing, and G. Zhou. isleep: unobtrusive sleep quality monitoring using smartphones. In *SenSys*, pages 4:1–4:14. ACM, 2013.

[7] M. Harville and D. Li. Fast, integrated person tracking and activity recognition with plan-view templates from a single stereo camera. In *CVPR 2004.*, volume 2, pages II–398. IEEE, 2004.

[8] Jawbone. UP. `https://jawbone.com/up`, 2014. [Online; accessed 28-Agust-2014].

[9] O. Kaltiokallio, M. Bocca, and N. Patwari. Enhancing the accuracy of radio tomographic imaging using channel diversity. In *IEEE MASS 2012*, pages 254–262. IEEE, 2012.

[10] M. Keally, G. Zhou, G. Xing, J. Wu, and A. Pyles. PBN: towards practical activity recognition using smartphone-based body sensor networks. In *SenSys*, pages 246–259. ACM, 2011.

[11] B. Kellogg, V. Talla, and S. Gollakota. Bringing gesture recognition to all devices. In *NSDI 14*, Seattle, WA, 2014. USENIX.

[12] J. R. Kwapisz, G. M. Weiss, and S. A. Moore. Activity recognition using cell phone accelerometers. *ACM SigKDD Explorations Newsletter*, 12(2):74–82, 2011.

[13] Leap Motion Inc. Leap motion. `https://www.leapmotion.com/`, 2014. [Online; accessed 15-September-2014].

[14] X. Mei and H. Ling. Robust visual tracking and vehicle classification via sparse representation. *IEEE TPAMI*, 33(11):2259–2272, 2011.

[15] P. Melgarejo, X. Zhang, P. Ramanathan, and D. Chu. Leveraging directional antenna capabilities for fine-grained gesture recognition. In *UbiComp '14*, pages 541–551, New York, NY, USA, 2014. ACM.

[16] Microsoft. Kinect. `http://www.microsoft.com/en-us/kinectforwindows/`, 2014. [Online; accessed 28-Agust-2014].

[17] P. Misra, W. Hu, M. Yang, and S. Jha. Efficient cross-correlation via sparse representation in sensor networks. In *IPSN 2012*, pages 13–24, New York, NY, USA, 2012. ACM.

[18] P. K. Misra, W. Hu, Y. Jin, J. Liu, A. Souza de Paula, N. Wirstrom, and T. Voigt. Energy efficient GPS acquisition with sparse-GPS. In *IPSN 2014*, pages 155–166. IEEE Press, 2014.

[19] N. Oliver, E. Horvitz, and A. Garg. Layered representations for human activity recognition. In *ICMI 2002*, pages 3–8. IEEE, 2002.

[20] Q. Pu, S. Gupta, S. Gollakota, and S. Patel. Whole-home gesture recognition using wireless signals. In *MobiCom 2013*, pages 27–38, Sept. 2013.

[21] N. Ravi, N. Dandekar, P. Mysore, and M. L. Littman. Activity recognition from accelerometer data. In *AAAI*, volume 5, pages 1541–1546, 2005.

[22] T. Sathyan, D. Humphrey, and M. Hedley. WASP: A system and algorithms for accurate radio localization using low-cost hardware. *Systems, Man, and Cybernetics, Part C: Applications and Reviews, IEEE Transactions on*, 41(2):211–222, 2011.

[23] S. Sen, J. Lee, K.-H. Kim, and P. Congdon. Avoiding multipath to revive inbuilding wifi localization. In *MobiSys 2013*, pages 249–262. ACM, 2013.

[24] S. Sen, B. Radunovic, R. R. Choudhury, and T. Minka. You are facing the Mona Lisa: spot localization using PHY layer information. In *MobiSys 2012*, pages 183–196. ACM, 2012.

[25] Y. Shen, W. Hu, J. Liu, M. Yang, B. Wei, and C. T. Chou. Efficient background subtraction for real-time tracking in embedded camera networks. In *SenSys '12*, pages 295–308, New York, NY, USA, 2012. ACM.

[26] Y. Shen, W. Hu, M. Yang, B. Wei, S. Lucey, and C. T. Chou. Face recognition on smartphones via optimised sparse representation classification. In *IPSN '14*, pages 237–248, Piscataway, NJ, USA, 2014. IEEE Press.

[27] S. Sigg, M. Scholz, S. Shi, Y. Ji, and M. Beigl. RF-sensing of activities from non-cooperative subjects in device-free recognition systems using ambient and local signals. *IEEE TMC*, 13(4):907–920, 2014.

[28] G. Wang, Y. Zou, Z. Zhou, K. Wu, and L. M. Ni. We can hear you with Wi-Fi! In *MobiCom 2014*, pages 593–604. ACM, 2014.

[29] Y. Wang, J. Liu, Y. Chen, M. Gruteser, J. Yang, and H. Liu. E-eyes: device-free location-oriented activity identification using fine-grained wifi signatures. In *MobiCom 2014*, pages 617–628. ACM, 2014.

[30] B. Wei, A. Varshney, N. Patwari, W. Hu, T. Voigt, Chou, and C. Tung. drti: Directional radio tomography. In *IPSN '15*, Seattle, WA, USA, 2015. ACM.

[31] B. Wei, M. Yang, Y. Shen, R. Rana, C. T. Chou, and W. Hu. Real-time classification via sparse representation in acoustic sensor networks. In *SenSys 2013*, page 21. ACM, 2013.

[32] J. Wilson and N. Patwari. Radio tomographic imaging with wireless networks. *IEEE TMC*, 9(5):621–632, 2010.

[33] J. Wright, A. Yang, A. Ganesh, S. Sastry, and Y. Ma. face recognition via sparse representation. *TPAMI*, 31(2):210–227, 2009.

[34] X. Wu and M. Liu. In-situ soil moisture sensing: Measurement scheduling and estimation using compressive sensing. In *IPSN '12*, pages 1–12, New York, NY, USA, 2012. ACM.

[35] Xiaomi. Mi Band. `http://www.mi.com/shouhuan`, 2014. [Online; accessed 28-August-2014].

[36] C. Xu, B. Firner, R. S. Moore, Y. Zhang, W. Trappe, R. Howard, F. Zhang, and N. An. Scpl: Indoor device-free multi-subject counting and localization using radio signal strength. In *IPSN '13*, pages 79–90, New York, NY, USA, 2013. ACM.

[37] C. Xu, B. Firner, Y. Zhang, R. Howard, J. Li, and X. Lin. Improving rf-based device-free passive localization in cluttered indoor environments through probabilistic classification methods. In *IPSN '12*, pages 209–220, New York, NY, USA, 2012. ACM.

[38] C. Xu, M. Gao, B. Firner, Y. Zhang, R. Howard, and J. Li. Towards robust device-free passive localization through automatic camera-assisted recalibration. In *ACM SenSys*, 2012.

[39] Z. Yang, Z. Zhou, and Y. Liu. From RSSI to CSI: Indoor localization via channel response. *ACM Comput. Surv.*, 46(2):25:1–25:32, Dec. 2013.

[40] K. Yatani and K. N. Truong. Bodyscope: a wearable acoustic sensor for activity recognition. In *Ubicomp 2012*, pages 341–350. ACM, 2012.

[41] M. Youssef, M. Mah, and A. Agrawala. Challenges: device-free passive localization for wireless environments. In *MobiCom 2007*, pages 222–229. ACM, 2007.

[42] T. Zhao, M. Aggarwal, R. Kumar, and H. Sawhney. Real-time wide area multi-camera stereo tracking. In *CVPR 2005*, volume 1, pages 976–983. IEEE, 2005.

[43] Y. Zhao and N. Patwari. Noise reduction for variance-based device-free localization and tracking. In *SECON 2011*, pages 179–187, 2011.

[44] Y. Zhao, N. Patwari, J. M. Phillips, and S. Venkatasubramanian. Radio tomographic imaging and tracking of stationary and moving people via kernel distance. In *IPSN '13*, pages 229–240, New York, NY, USA, 2013. ACM.

[45] Z. Zhou, Z. Yang, C. Wu, L. Shangguan, and Y. Liu. Omnidirectional coverage for device-free passive human detection. *IEEE TPDS*, 2013.